1000–1007 *Nucleic Acids Research, 1996, Vol. 24, No. 6*

The *cis*-acting elements involved in endonucleolytic cleavage of the 3′ UTR of human IGF-II mRNAs bind a 50 kDa protein

Wiep Scheper*, P. Elly Holthuizen and John S. Sussenbach

Laboratory for Physiological Chemistry, Graduate School of Developmental Biology, Utrecht University, PO Box 80042, 3508 TA Utrecht, The Netherlands

Received January 8, 1996; Revised and Accepted February 8, 1996

ABSTRACT

Site-specific cleavage of human insulin-like growth factor II mRNAs requires two *cis*-acting elements, I and II, that are both located in the 3′ untranslated region and separated by almost 2 kb. These elements can interact and form a stable RNA–RNA stem structure. In this study we have initiated the investigation of *trans*-acting factors involved in the cleavage of IGF-II mRNAs. The products of the cleavage reaction accumulate in the cytoplasm, suggesting that cleavage occurs in this cellular compartment. By electrophoretic mobility shift assays, we have identified a cytoplasmic protein with an apparent molecular weight of 48–50 kDa, IGF-II cleavage unit binding protein (ICU-BP), that binds to the stem structure formed by interaction of parts of the *cis*-acting elements I and II. The binding is resistant to high K^+ concentrations and is dependent on Mg^{2+}. In addition, ICU-BP binding is dependent on the cell density and correlates inversely with the IGF-II mRNA levels. *In vivo* cross-linking data show that this protein is associated with IGF-II mRNAs *in vivo*.

INTRODUCTION

Human insulin-like growth factor II (IGF-II) is encoded by a single gene that contains four promoters P1–P4 which give rise to a family of mRNAs. These promoters are differentially active in a tissue- and development-specific manner and render mRNAs of 5.3 (P1), 5.0 (P2), 6.0 (P3) and 4.8 kb (P4) respectively (1). The transcripts share the IGF-II coding region, but have different 5′ untranslated regions (UTRs), leading to differential translatability (2,3). All IGF-II mRNAs are targets for site-specific endonucleolytic cleavage in the 4.2 kb 3′UTR, rendering an unstable capped 5′ cleavage product containing the coding region and an unusually stable polyadenylated 3′ cleavage product of 1.8 kb consisting of the 3′ terminal region of the 3′UTR (4).

The importance of RNA processing as a regulatory level in the control of gene expression becomes increasingly appreciated as more insight into post-transcriptional events is generated (5–7). Analysis of nuclear RNA-processing events has revealed many details of both pre-mRNA splicing (8) and 3′ end formation (9). In contrast, relatively little is known about the processing of mature mRNAs in eukaryotes, not in the least because of the difficulties in establishing *in vitro* degradation assays. It is clear that in these processes, *cis*-acting elements in the mRNA interact with specific *trans*-acting factors. In yeast cells, some of the mRNA degradation pathways are being elucidated, and genetic screens have allowed the identification of different *trans*-acting factors (reviewed in 6). Mammals do not allow a genetic analysis and the identification of *trans*-acting factors has to start with biochemical rather than genetic approaches. Many of the mammalian *trans*-acting factors have been identified based on their ability to bind to *cis*-acting elements in certain mRNAs (10–16). Due to the structural versatility of RNA, binding of RNA by RNA-binding proteins is often dependent on both sequence- and structure-specific recognition, e.g. iron-responsive element binding protein (IRP) binding to the iron-responsive element (IRE) (17), human immuno deficiency virus (HIV) Tat protein to the Tar region (18) and HIV Rev to the Rev response element (RRE) (19).

Previously, we have identified two *cis*-acting elements in the 3′-UTR that are required for cleavage of IGF-II mRNAs (20,21). These two elements are separated by approximately 2 kb that can be deleted without decreasing the cleavage efficiency. Element I is located at positions –2116/–2013 and contains no obvious features in its primary sequence or secondary structure. Element II at –173/+150 encompasses the cleavage site and contains two regions that are highly conserved among human, rat and mouse (20): two stem–loops upstream of the cleavage site (–139/–3) and a G-rich region at positions –14/+60 (positions are relative to the cleavage site which is set to +1; Fig. 1A). Cleavage *in vivo* requires the presence of an intact cleavage unit comprising both elements (Fig. 1B). Site-specific endonucleolytic cleavage of IGF-II mRNAs is unique since, firstly, the two *cis*-acting elements are so widely separated from each other, and, secondly, the sizes of these elements are very large. We have shown that a region of element I (–2108/–2029) and a region in element II downstream of the cleavage site (+18/+101) form a very stable stem structure (Fig. 1B), that is conserved among human, rat and mouse IGF-II mRNAs. In addition, our data clearly indicate that both the secondary structure and the sequence of this stem structure are important for cleavage (21). This suggests that elements I and II

* To whom correspondence should be addressed

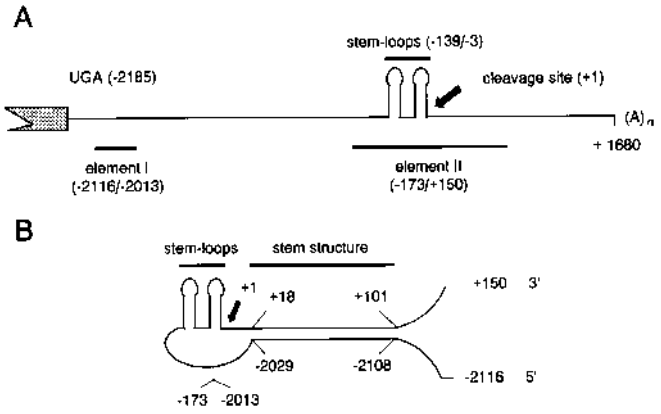

Figure 1. Location of the *cis*-acting elements involved in cleavage of IGF-II mRNAs. (**A**) Schematic representation of the positions of the *cis*-acting elements involved in endonucleolytic cleavage in the 3′ UTR of IGF-II mRNAs. Positions in exon 9 of the human IGF-II gene are indicated relative to the cleavage site, which is set to +1. The stop codon of the IGF-II open reading frame is located at position –2185. Elements I and II are separated by ~2 kb (drawing not to scale). Element II encompasses two stem–loops (–139/–3), the cleavage site (+1) and a G-rich region at positions –14/+60 which is highly conserved among human, rat and mouse (20). (**B**) Schematic representation of the structure of the minimal cleavage unit. As was shown previously, the region between elements I and II (–2012/–174) can be deleted without disrupting the cleavage reaction and efficiency (20). Indicated are the stem structure that is formed by an interaction of element I (–2108/–2029) and element II (+18/+101), the two stem–loops (–139/–3) in element II and the cleavage site (+1).

cooperate in the binding of *trans*-acting factors involved in cleavage of IGF-II mRNAs. The identification of proteins binding to the *cis*-acting elements required for cleavage may provide critical insight into the mechanism underlying the specific endonucleolytic cleavage of IGF-II mRNAs. In the present study we have initiated the identification of *trans*-acting factors that interact with the IGF-II cleavage unit.

MATERIALS AND METHODS

Materials

Plasmid pBluescript II (KS^+) was obtained from Stratagene (La Jolla, CA). Enzymes were purchased from Boehringer Mannheim (Germany), with the exception of Pfu DNA polymerase (Stratagene, La Jolla, CA), RNase-free DNase (Promega, Madison, WI) and RNase T1 (CalBiochem, La Jolla, CA). Enzymes were used according to the manufacturer's instructions. NTPs and dNTPs were obtained from Kabi-Pharmacia (Uppsala, Sweden). G418 was purchased from Sigma (St Louis, MO). A random priming DNA labeling kit was purchased from Boehringer Mannheim (Germany) and a DNA sequencing kit from Kabi-Pharmacia (Uppsala, Sweden). Guanidinium thiocyanate was obtained from Fluka (Buchs, Switzerland) and GeneScreen membranes from Du Pont de Nemours (Dreiech, Germany). [α-^{32}P]dCTP (3000 Ci/mmol) and [α-^{32}P]CTP (760 Ci/mmol) were purchased from Amersham (Buckinghamshire, UK).

Cell culture, extract preparation and *in vivo* cross-linking

The cell lines HeLa and Ltk$^-$ were grown in Dulbecco's Modified Eagle's Medium (DMEM), the stable Ltk$^-$ cell line EP7-9 (22) was grown in the DMEM in the presence of 300 μg/ml G418 and Hep3B cells were grown in α-Minimal Essential Medium (α-MEM). All media were supplemented with 10% fetal calf serum, 100 IU/ml penicillin, 100 μg/μl streptomycin and 300 μg/ml glutamine.

Cytoplasmic and nuclear cell fractions were prepared employing a method adapted from Vakalopoulou *et al.* (12) with slight modifications. Briefly, the cells were lysed in 10 mM Tris pH 8.0, 10 mM NaCl, 3 mM $MgCl_2$, 1 mM DTT, 1 mM phenylmethylsulphonic acid, 0.5% NP-40 and 0.5% sodium deoxycholate on ice for 10 min. Subsequently, the lysate was spun in a microfuge for 5 min at 4°C and the supernatant was collected and used for cytoplasmic RNA isolation or stored at –80°C in 10% glycerol (cytoplasmic extract). The pellet was used to isolate nuclear RNA or to prepare nuclear extracts as described in (23). Protein concentrations were determined by the Bradford protein assay (BioRad, München, Germany).

In vivo cross-linking experiments were performed essentially as in (24). Briefly, cells were grown on 100 mm plates, washed twice with cold PBS and exposed to UV light (254 nm) at 1.9 J/cm^2 (Stratalinker, Stratagene, La Jolla, CA) in 5 ml PBS on ice prior to preparation of the extracts.

Cellular RNA isolation and analysis

RNA was isolated from the cytoplasmic, nuclear and total cell fractions by the single-step guanidinium thiocyanate method (25). RNA (10 μg) was glyoxalated and size-separated on a 1% agarose 10 mM sodium phosphate gel and transferred to a GeneScreen membrane. The RNA was fixed on the membrane by irradiation with long-wavelength UV light for 2.5 min and baking at 80°C for 2 h. Northern blots were hybridized in the presence of 50% formamide according to GeneScreen protocols in glass cylinders with continuous rotation at 42°C. DNA fragments were labeled by random priming with [α-^{32}P]dCTP and added after 3 h prehybridization at a final concentration of 10^6 c.p.m./ml. After overnight hybridization, blots were washed to a final stringency of 0.5 or 0.1× SSC, 1% SDS at 65°C (1× SSC is 0.15 M NaCl, 0.015 M sodium citrate) and exposed on Fuji RX X-ray film. Two human IGF-II exon 9 probes were used: a 532 bp *Eco*RV–*Ava*I fragment encompassing the region between positions –557 and –26 (5′-specific probe) and a 1.0 kb *Sma*I fragment (positions +81/+1094; 3′-specific probe). A 26 nt-long oligonucleotide was used as a 28S ribosomal probe: 5′-AACGATCAGAGTAGTGGTATTTCACC-3′. Hybridization conditions for this probe were identical to the IGF-II probe except for the formamide concentration (25%). Blots were washed for 30 min in 2× SSC, 1% SDS and 30 min in 1× SSC, 1% SDS at 30°C. The autoradiographs were analyzed by densitometric scannning.

Construction of plasmids

For the preparation of BS-S/S, BS-AS/S and BS-AS/AS (Fig. 6A), oligonucleotides 5′ *Bam*HI –2340/–2334 3′ and 5′ *Eco*RI +169/+151 3′ (numbers indicate positions in exon 9) were used as primers in PCR reactions on plasmids S/S, AS/S and AS/AS respectively. The latter constructs are IGF-II expression plasmids containing elements I/II in the sense (S) or antisense (AS) orientation as indicated and are described in detail in (21). The PCR products were subcloned in the *Bam*HI and *Eco*RI sites of pBluescript KS^+, resulting in the plasmids BS-S/S, BS-AS/S and BS-AS/AS. BS-II was prepared by PCR with primers 5′ *Bam*H1 –173/–155 3′ and 5′ *Eco*RI +169/+151 3′ on S/S. BS-AS/ASΔ was prepared from BS-AS/AS by replacing the *Bgl*II (–110)–*Eco*RI

(+170) fragment with a PCR product made with primers 5′ *Bgl*II –14/+4 3′ and 5′ *Eco*RI +169/+151 3′ on template BS-AS/AS, resulting in a deletion of nucleotides –104/–15 from BS-AS/AS. All constructs were checked by restriction enzyme analysis or sequencing if necessary.

Synthesis of RNA probes and competitors

Radiolabeled RNA probes and unlabeled competitor RNAs were synthesized using T7 RNA polymerase on linearized DNA templates according to instructions of the manufacturer in the presence of 1 mM ATP, GTP and UTP each and 20 µCi [α-^{32}P]CTP and 0.1 mM CTP (radiolabeled) or 1 mM CTP (unlabeled). Templates used for synthesis of the RNAs: I: BS-S/S linearized with *Bgl*II (–110), II: BS-II linearized with *Eco*RI, I/II: BS-S/S linearized with *Eco*RI, AS/S: BS-AS/S linearized with *Eco*RI, AS/AS: BS-AS/AS linearized with *Eco*RI, and AS/ASΔ: BS-AS/ASΔ linearized with *Eco*RI. After synthesis (1 h) the template was removed by DNase I treatment (1 U in 20 µl reaction mixture for 15 min at 37°C) and the RNA was separated from unincorporated nucleotides by Sephadex G25 spin dialysis. Subsequently, the samples were phenol/chloroform extracted, ethanol precipitated, washed in 70% ethanol and renatured in renaturation buffer (20 mM Tris–HCl pH 7.5, 100 mM KCl, 2 mM $MgCl_2$), 5 min at 90°C and 30 min on ice. The integrity of the RNAs was checked by gel electrophoresis.

Analysis of RNA–protein interactions

For electrophoretic mobility shift assays (EMSAs), radiolabeled RNA probes (10^5 c.p.m.) were incubated in cellular extract with a protein content of 10 µg in a 10 µl reaction mixture containing 20 mM HEPES–KOH pH 7.5, 100 mM KCl, 1 mM $MgCl_2$, 1 mM DTT and 0.01% NP-40 for 45 min on ice. In competition experiments, the competitor RNAs were preincubated with the extract for 5 min before addition of the probe. After the binding reaction the samples were incubated at room temperature for 20 min with a mixture of 12.5 µg/ml RNase A and 2 U/ml RNase T1. Samples were analyzed on a non-denaturing 6% polyacrylamide gel containing 0.01% NP-40.

The molecular weight of IGF-II cleavage unit binding protein (ICU-BP) was determined as described in (26). First the IGF-II cleavage unit RNA–protein complex (ICU-RPC) was UV cross-linked in an EMSA gel (254 nm, 5 J/cm^2) and a gel slice containing this complex (localized by wet gel autoradiography) was excised. Subsequently the gel slice was inserted into a 10% SDS–PAGE gel and electrophoresed with ^{14}C-methylated protein markers (Amersham, Buckinghamshire, UK) loaded in parallel.

RESULTS

Subcellular localization of the cleavage reaction site

To investigate whether cleavage of IGF-II mRNAs takes place in a particular subcellular compartment, 10 µg cytoplasmic or nuclear RNA from Hep3B cells were analyzed by Northern blotting (Fig. 2). Hep3B is a human hepatoma cell line that endogenously expresses both the 6.0 and the 4.8 kb mRNAs derived from promoters P3 and P4, respectively. The full-length mRNAs are present in comparable amounts in both the cytoplasmic and nuclear fractions. Cleavage of these mRNAs renders a polyadenylated 3′ cleavage product of 1.8 kb that hybridizes exclusively with the 3′-specific IGF-II exon 9 probe. The capped 5′ cleavage product derived from the 6.0 kb mRNA, with a size of 4.2 kb, is detected by the 5′-specific probe. The amount of 5′ cleavage product of the 4.8 kb mRNA is below the detection level, probably due to the low relative levels of this mRNA species. In contrast with the full-length IGF-II mRNAs, the 3′ and 5′ cleavage products are readily detected in the cytoplasmic RNA fraction, but not in the nuclear fraction (Fig. 2). The cytoplasmic localization of the cleavage products becomes even more pronounced if we take into consideration that equal amounts of RNA were loaded for each fraction, but that 10 µg nuclear RNA is derived from eight times more cells than 10 µg cytoplasmic RNA. Obviously, the cleavage products accumulate in the cytoplasm, suggesting that cleavage takes place in the cytoplasm, although nuclear cleavage and rapid transport can not be fully excluded.

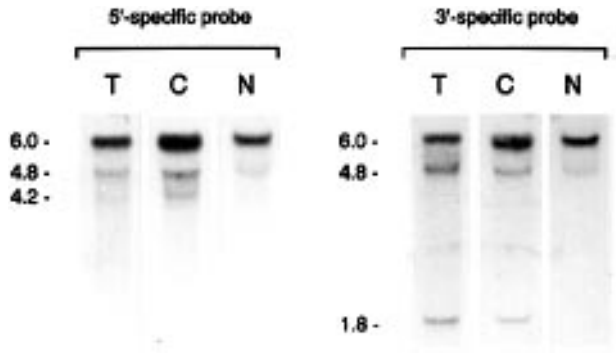

Figure 2. Subcellular localization of the cleavage products. Northern blot analysis of total (T), cytoplasmic (C) and nuclear (N) RNA isolated from Hep3B cells, 10 µg RNA was loaded in each lane. The blot was hybridized with two IGF-II exon 9 probes. The 5′-specific probe (–557/–26) detects full-length IGF-II transcripts and the 5′ cleavage product of 4.2 kb; the 3′-specific probe (+81/+1094) detects full-length IGF-II mRNAs and the 3′ cleavage product of 1.8 kb. Positions are relative to the cleavage site, which is set to +1. Sizes of the RNAs are indicated in kb.

If cleavage is a cytoplasmic event, this would suggest that the *trans*-acting factors involved in this process may be localized in the cytoplasm. Cleavage of IGF-II mRNAs requires the presence of a cleavage unit (elements I and II; Fig. 1B). To identify *trans*-acting factors binding to this cleavage unit, EMSAs were performed with a probe containing the intact cleavage unit (I/II) and cytoplasmic or nuclear extracts from Hep3B cells that endogenously express IGF-II mRNAs (Fig. 2). A major complex designated ICU-RPC (IGF-II cleavage unit RNA–protein complex) is detected that is highly enriched in the cytoplasm (Fig. 3). We focused on ICU-RPC, because this RNA–protein complex is enriched in the cytoplasm and is common among different cell lines that are capable of cleavage. Both cytoplasmic extracts from the IGF-II mRNAs expressing Hep3B cells, as well as extracts from Ltk$^-$ and HeLa cells which do not endogenously express IGF-II, but are able to cleave mRNAs derived from a transfected IGF-II minigene, give rise to the formation of ICU-RPC (Figs 3, 4 and 7).

Characteristics of the RNA–protein complex

To examine further the specific mRNA–protein interaction and to characterize the protein components of ICU-RPC, we cross-linked ICU-RPC in a gel and subsequently inserted the gel slice containing the cross-linked complex into a 10% SDS–PAGE gel (see Materials and Methods for details). This analysis revealed that

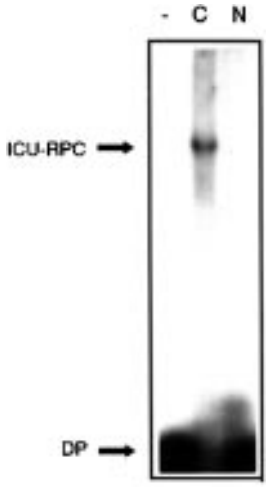

Figure 3. Identification of proteins interacting with the cleavage unit. Electrophoretic mobility shift assay of a ^{32}P-labeled RNA probe, I/II, consisting of the cleavage unit (schematically represented in Fig. 1B), without extract (–), with 10 µg cytoplasmic (C) or 10 µg nuclear (N) extract from Hep3B cells respectively. The binding reaction was performed on ice for 45 min. Samples were digested with RNase A and RNase T1 before loading onto a 6% non-denaturing polyacrylamide gel. The IGF-II cleavage unit RNA–protein complex is designated ICU-RPC; digested probe is indicated by DP.

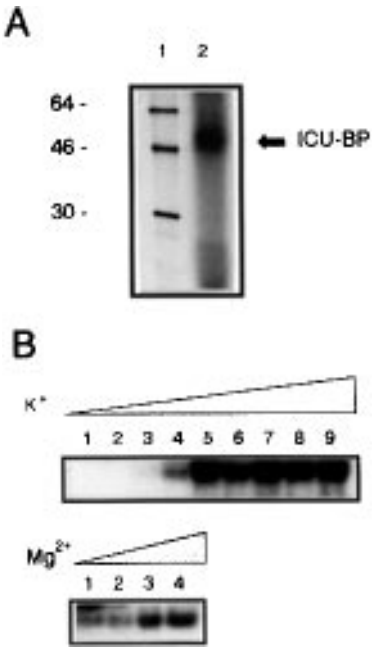

Figure 4. Characteristics of ICU-RPC. (**A**) Size determination of the protein component of the RNA–protein complex ICU-RPC. ^{32}P-labeled RNA was incubated with HeLa cytoplasmic extract, RNase treated, and run on a non-denaturing gel. Subsequently the gel was UV irradiated. The specific RNA–protein complex ICU-RPC was then removed from the gel and subsequently analyzed by electrophoresis on a 10% SDS–PAGE gel (lane 2). The apparent size of the protein, designated IGF-II cleavage unit binding protein (ICU-BP) was determined at 48–50 kDa. The sizes of ^{14}C-labeled molecular weight markers (lane 1) are indicated on the left in kDa. (**B**) Electrophoretic mobility shift analysis of ^{32}P-labeled RNA probe I/II with 10 µg HeLa cytoplasmic extract; only the ICU-RPC is shown. Upper panel: effect of increasing amounts of KCl added to the binding reaction mixture. From lanes 1 to 9, the KCl concentration is 10, 25, 50, 75, 100, 150, 200, 400 and 600 mM respectively. Lower panel: effect of increasing amounts of $MgCl_2$ added to the binding reaction mixture. Lane 1: no $MgCl_2$ and 10 mM EDTA. The samples in lanes 2, 3 and 4 contain 1, 10 and 100 mM $MgCl_2$ respectively.

the protein binding to the cleavage unit has an apparent molecular weight of 48–50 kDa (Fig. 4A). Since the formation of ICU-RPC is abolished by proteinase K pretreatment of the extract, but not by Micrococcal Nuclease pretreatment (data not shown), ICU-RPC does not require a nucleic acid component from the extract. Obviously, the 48–50 kDa protein is the main protein component in ICU-RPC. We will refer to this protein as ICU-BP (IGF-II cleavage unit binding protein).

Interactions of proteins with nucleic acids are highly dependent on the salt concentrations. Therefore, we analyzed the binding capacity of ICU-BP in the presence of increasing K^+ concentrations. ICU-BP does not bind at very low K^+ concentrations (Fig. 4B), but binds efficiently at physiological K^+ concentrations and still forms a stable RNA–protein complex in 600 mM KCl. Divalent cations play an important role in many cellular processes. When divalent cations are chelated from the binding buffer by EDTA, binding of ICU-BP is strongly decreased. This inhibition can be overcome by Mg^{2+}, and high concentrations of these ions increase the binding. The physiological binding conditions used throughout our binding studies (100 mM KCl, 1 mM Mg^{2+}) are obviously favourable for ICU-BP binding.

Elements I and II cooperate in binding of ICU-BP

We have shown previously that the *cis*-acting elements I and II are both required for cleavage. Parts of these elements form a long stem structure that stabilizes two additional stem–loops upstream of the cleavage site in element II, as was shown by RNase T1 digestion experiments (Fig. 1B; 21). In addition, we showed that the stem structure functions in a sequence-specific manner (21), suggesting that recognition of the stem structure by *trans*-acting factors is important for cleavage. To investigate whether ICU-BP is involved in recognition of the stem structure, the requirements for ICU-BP binding were analyzed using different probes in an EMSA (Fig. 5A). First we analyzed the binding of ICU-BP to probes consisting of elements I or II separately (probes I and II respectively), and compared this with probe I/II that contains both elements (Fig. 5B). ICU-RPC is not formed when either probe I or probe II is used, but only when both elements are present, indicating that the elements cooperate in binding of ICU-BP. In competition experiments with unlabeled competitor RNAs, the ICU-BP binding is competed very efficiently by the cleavage unit RNA (I/II) (Fig. 5C). Competition is almost complete already at the lowest competitor concentration (10 ng/binding mixture). The individual elements I and II can only compete when present in higher excess, probably because at these higher concentrations (50–100 ng/binding mixture) they interact with the probe. Yeast tRNA does not compete with I/II for binding, but instead the binding increases at higher concentrations of tRNA, most likely caused by sequestration of non-specific factors that interfere with the formation of specific RNA–protein complexes.

The formation of ICU-BP–RNA complex requires both elements (Fig. 5). This could mean that (i) ICU-BP binds the stem structure that can be formed between elements I and II, or (ii) ICU-BP binds the two stem–loops upstream of the cleavage site in element II, that are stabilized by the interaction between elements I and II (21). To discriminate between these possibilities, we used

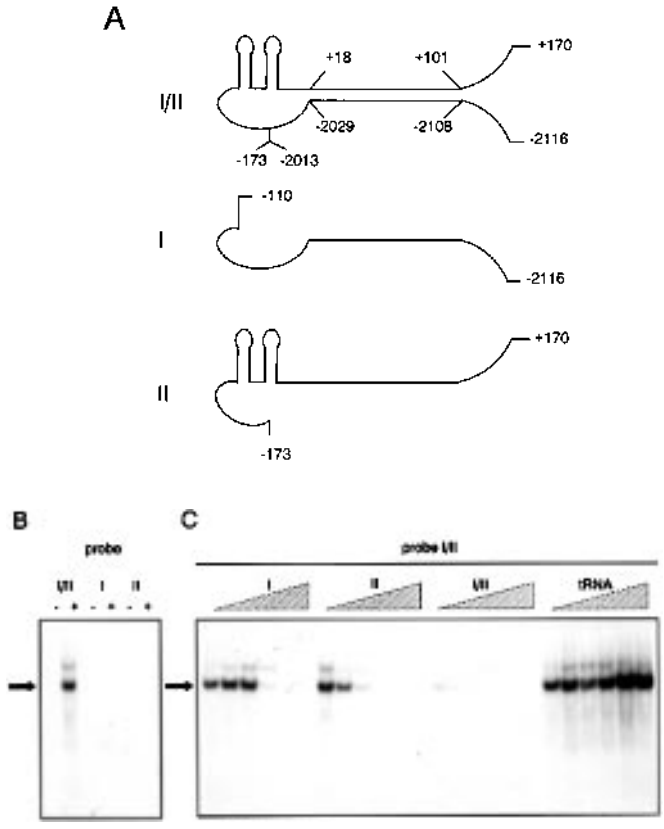

Figure 5. Analysis of the ICU-RPC formation with elements I and II. (**A**) Schematic representation of the probes used in the electrophoretic mobility shift assay. I/II: intact cleavage unit; I: separate element I; II: separate element II. Numbers indicate the positions in IGF-II exon 9 relative to the cleavage site (+1). (**B**) Electrophoretic mobility shift analysis of ^{32}P-labeled RNA probes as depicted in (A), in the presence (+) or absence (–) of 10 µg HeLa cytoplasmic extract. The binding reaction was performed on ice for 45 min. Samples were digested with RNase A and RNase T1 before loading onto a 6% non-denaturing polyacrylamide gel. The position of the ICU-RPC is indicated by an arrow. (**C**) Competition electrophoretic mobility shift analysis of ^{32}P-labeled RNA probe I/II and 10 µg HeLa cytoplasmic extract. Unlabeled competitor RNAs were added to the reaction mixture in increasing amounts of 10, 25, 50, 100, 250 and 500 ng respectively, as indicated by the hatched wedges. Competitors used: the single elements I or II, the cleavage unit I/II itself, or non-specific yeast tRNA. The arrow designates the position of the ICU-RPC.

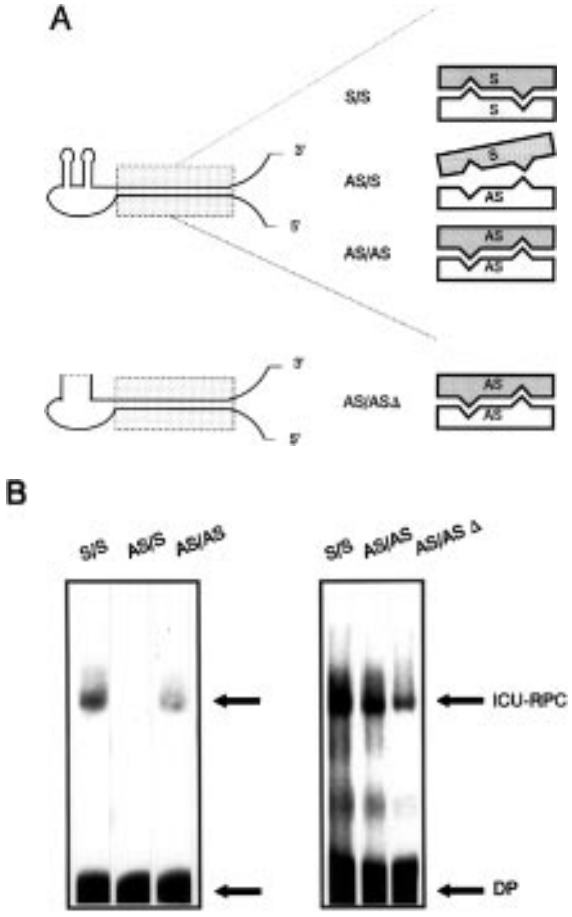

Figure 6. Analysis of ICU-RPC formation with stem structure mutants. (**A**) Schematic representation of the configuration mutants. These mutants are derivatives of I/II (S/S). In the left hand panel the overall structure of the probes is drawn, and in the right hand panel the stem structure between elements I and II is shown enlarged. The different orientations of the two parts of the stem structure are indicated by S (sense) and AS (antisense). The deletion of the stem–loops in element II from AS/AS is also indicated; the linkage of the regions flanking the deletion is indicated by a dashed line. (**B**) Electrophoretic mobility shift analysis of ^{32}P-labeled RNA probes as depicted in A with 10 µg Hep3B cytoplasmic extract. Left panel: RNA probes S/S, AS/S and AS/AS respectively. Right panel: RNA probes S/S, AS/AS and AS/ASΔ respectively. The complex ICU-RPC is indicated by an arrow, as well as the digested probe (DP).

mutant cleavage units containing different configurations of the stem structure as probes in an EMSA experiment (Fig. 6). These mutants contain the two parts of the stem structure in either the sense (S) or antisense (AS) orientation. Wild-type S/S RNA (identical to I/II) was compared with AS/S RNA containing element I in the antisense orientation thereby disrupting the stem structure, and AS/AS RNA in which the stem structure is restored by compensatory mutations in element II. The mutations are exclusively in the stem structure regions leaving both the stem–loops in element II and the cleavage site intact (Fig. 6A). Figure 6B shows that ICU-BP can bind to the S/S configuration, but does not bind to the AS/S RNA. Furthermore, the AS/AS configuration does give rise to formation of the ICU-BP–RNA complex, albeit with somewhat lower efficiency. It appears that the AS/S RNA can not form the complex, whereas the S/S and AS/AS RNAs can, which confirms that interaction between the elements is required for binding. However, this result still does not discriminate between the binding of ICU-BP to the stem structure itself or binding to the two stem–loops. If the binding-site for ICU-BP is located in the stem structure, the AS/AS stem structure by itself should be able to bind ICU-BP. Therefore, the two stem–loops were deleted from the AS/AS RNA, leaving only the stem structure between the elements (AS/ASΔ). Figure 6B clearly demonstrates that also the AS/ASΔ RNA gives rise to formation of the complex, albeit with a somewhat lower efficiency. This indicates that the binding site for ICU-BP is predominantly located in the stem region (–2108/–2029 and +18/+101), and not in the two additional stem–loops of element II.

Regulation of ICU-BP binding

If binding of ICU-BP is involved in cleavage of IGF-II mRNAs, it may be expected that its binding is regulated in a manner that correlates with the expression pattern of IGF-II. Cytoplasmic

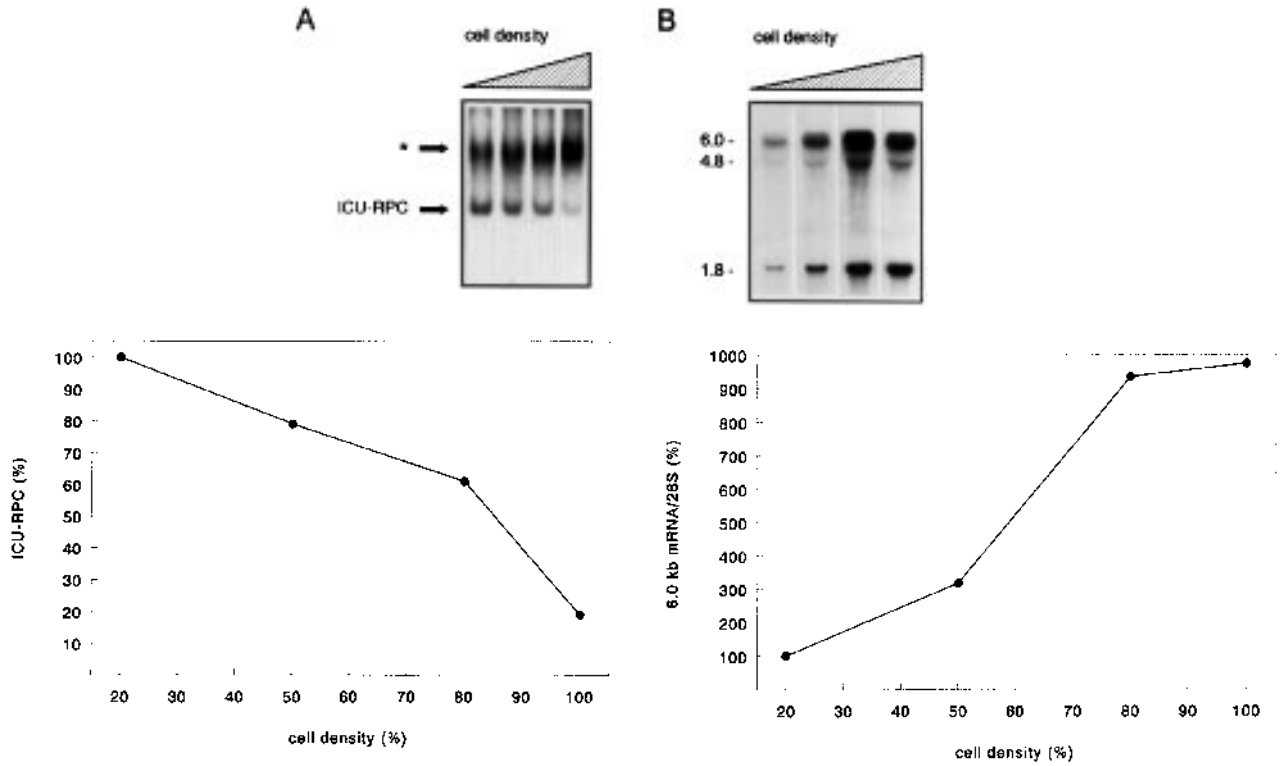

Figure 7. ICU-BP binding and IGF-II mRNA levels are inversely correlated. (**A**) Electrophoretic mobility shift analysis of probe I/II with cytoplasmic extract from Hep3B cells grown at increasing densities (20, 50, 80 and 100% respectively). The complex ICU-RPC is indicated by an arrow. The lower mobility complex that is enriched in confluent cells is indicated by an asterix. At the bottom, quantification of the ICU-RPC level is shown in a graph, the ICU-RPC level at cell density of 20% was set at 100%. (**B**) Northern blot analysis of total RNA isolated from Hep3B cells grown at increasing densities (20, 50, 80 and 100% respectively). In each lane, 10 µg RNA was loaded and the blot was hybridized with the 3′-specific probe (+81/+1094) that detects full length IGF-II mRNAs and the 3′ cleavage product of 1.8 kb. Positions are relative to the cleavage site, which is set to +1. Sizes of the RNAs are indicated in kb. RNA loading differences were normalized after hybridization with a 28S ribosomal probe. The normalized 6.0 kb mRNA levels are indicated in the graph below, the 6.0 kb mRNA level at a cell density of 20% was set at 100%.

extracts were prepared from Hep3B cells grown at various densities (20, 50, 80 and 100%) and tested in an EMSA with probe I/II (Fig. 7A). In extract from exponentially growing cells (20%), ICU-RPC is prominently present. In contrast, in extract from the confluent cells (100%), the complex formation is strongly decreased. Densitometric scanning of the autoradiogram shows a gradual decrease of ICU-RPC upon increasing cell density. This results in a 5-fold reduction of ICU-RPC formation when 20 and 100% confluent cells are compared, and the total amount of protein used for the EMSA is identical (Fig. 7A). In parallel with the decrease of ICU-RPC formation with increasing cell density, a yet unidentified lower mobility complex appears (indicated by an asterix). In parallel total RNA was isolated from dishes with cells grown to the various cell densities and 10 µg of each sample was analyzed on a Northern blot. A strong increase in the levels of IGF-II mRNA in confluent cells is observed (Fig. 7B). Apparently this applies to both the 6.0 and 4.8 kb mRNAs as well as to the 1.8 kb cleavage product. The amount of the 6.0 kb major IGF-II transcript was quantified by densitometric scanning and normalized with a 28S ribosomal probe. The 6.0 kb mRNA level gradually rises with increasing cell densities up to 10-fold in confluent cells (Fig. 7B). These results indicate that the formation of ICU-RPC correlates inversely with the IGF-II mRNA level in Hep3B cells.

In vivo detection of the ICU-RPC cleavage unit RNA–protein complex

Various lines of evidence suggest a role for ICU-BP in cleavage of IGF-II mRNAs: (i) both the protein and the cleavage products are highly enriched in the cytoplasm; (ii) the protein binds to the *cis*-acting elements involved in cleavage; and (iii) the binding of the protein correlates inversely with the IGF-II mRNA levels. To demonstrate further that ICU-BP also specifically interacts *in vivo* with IGF-II mRNAs, the following experiment was performed. Two cell lines, untransfected Ltk$^-$ cells that do not express IGF-II mRNAs and Ltk$^-$ cells stably transfected with an IGF-II minigene EP7-9 (22), were irradiated with UV light. If ICU-BP is associated with IGF-II mRNAs *in vivo*, UV irradiation will cross-link the protein to the mRNAs, thereby preventing it from binding to radiolabeled I/II RNA after preparation of a cytoplasmic extract. As shown in Figure 8, ICU-BP is depleted from the Ltk$^-$ EP7-9 cell extract after the UV treatment, whereas no difference is observed in the untransfected Ltk$^-$ cells, although the protein yields from both lines are comparable. This indicates that the depletion is not due to non-specific cross-linking or artefactual damage to the complex, but that it is caused specifically by cross-linking the protein to the IGF-II mRNAs. These results demonstrate that

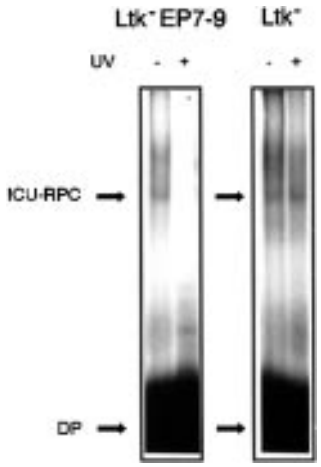

Figure 8. *In vivo* detection of the IGF-II cleavage unit RNA–protein complex. Ltk⁻ cells stably transfected with an IGF-II expression plasmid EP7-9, and non-transfected Ltk⁻ cells were UV-irradiated as described in Materials and Methods. Cytoplasmic extracts were prepared from the UV-irradiated cells as well as from non-UV-treated cells. Subsequently, an electrophoretic mobility shift analysis was performed of ^{32}P-labeled RNA probe I/II with 10 µg cytoplasmic extract of non-treated (–) or UV-irradiated (+) cells, both untransfected and EP7-9 transfected Ltk⁻ cells. The complex ICU-RPC is indicated by an arrow, as well as the digested probe (DP).

ICU-BP can also form a specific RNA–protein complex with IGF-II mRNAs *in vivo*.

DISCUSSION

Previously, we have identified two *cis*-acting elements required for cleavage of human IGF-II mRNAs (20) and we have demonstrated that part of these elements interact to form a stable stem structure and that in addition two stem–loops in element II are required for cleavage (21). In this report we have studied in which subcellular compartment the cleavage reaction takes place and initiated investigation of the *trans*-acting factors involved in cleavage. Processing of mature mRNAs predominantly occurs in the cytoplasm and since it was shown that the products of the cleavage reaction accumulate in the cytoplasm, it is likely that the IGF-II mRNA cleavage is also a cytoplasmic event. Although we can not formally exclude the possibility that both cleavage products are very rapidly exported from the nucleus to the cytoplasm after cleavage has occurred, the results strongly suggest that the cleavage reaction mainly, if not exclusively, takes place in the cytoplasm. Therefore, the *trans*-acting factors involved in cleavage are most likely localized in the cytoplasm. We have identified a novel RNA–protein complex (ICU-RPC) that forms on the cleavage unit and is strongly enriched in the cytoplasm. The major extract component of this complex is a protein with an apparent molecular weight of 48–50 kDa, which we named ICU-BP. The ICU-BP protein is present in both endogenously IGF-II expressing (Hep3B) and non-expressing cell lines (HeLa, Ltk⁻) and shows identical binding characteristics in these cells (data not shown). Similarly, the cleavage activity is not restricted to IGF-II expressing cells, because non-IGF-II expressing cell lines transfected with IGF-II mini-gene constructs are also able to cleave IGF-II mRNAs. Also, the fact that the RNA–protein complex is formed in both human (Hep3B, HeLa) and mouse (Ltk⁻) extracts is not surprising, because human mRNAs are cleaved efficiently in human cells as well as in mouse Ltk⁻ cells (22).

We used elements I and II of the cleavage unit separately in an EMSA and showed that binding of ICU-BP requires the presence of both elements. This by itself would not necessarily call for an interaction between the elements, but could be explained if the binding site would be partly located in element I and partly in element II. However, we used an element I probe that still contains the first 60 nt of element II that are not involved in stem structure formation and this did not bind. Furthermore, in the authentic IGF-II mRNAs elements I and II are separated by 2 kb. Additional evidence for the requirement for a cooperation of both elements was obtained by EMSA analysis with orientation mutants, showing that the AS/S RNA which can not form the stem structure does not bind ICU-BP, whereas the AS/AS RNA that forms a stem similar to the S/S RNA can bind ICU-BP. We have shown before that the presence of the stem structure stabilizes the two additional stem–loop structures in element II (21). Therefore, the results with the orientation mutants could also be explained if ICU-BP binds these stem–loops. The AS/ASΔ mutant which lacks the stem–loops, binds ICU-BP, albeit with a somewhat reduced efficiency. This shows that the binding site for ICU-BP is located in the stem structure and not in the two additional stem–loops of element II. Why is ICU-BP able to bind the AS/AS mutant stem structure, while this RNA is not a substrate for the cleavage reaction *in vivo*? The sequence from this mutant stem is of course very similar to the wild-type stem (21) and apparently the information suffices for binding, but not for cleavage. It is possible that this is merely an orientation effect, since the main difference between the AS/AS RNA and the S/S RNA is the orientation of the stem structure relative to the cleavage site. It has been reported before that mRNA binding capacity and activity of a protein can be separated. Proteinase K abolishes the c-*myc* mRNA *in vitro* degradation without affecting the binding to the AU-rich element in the c-*myc* mRNA (27).

In summary, these data indicate that ICU-BP recognizes the stem structure formed between the regions of elements I and II located at –2108/–2029 and +18/+101. Previous results showed that this stem structure functions in a sequence-specific manner in cleavage (as was shown for the HIV Rev protein recognition; 19), thereby suggesting that it is a target for a *trans*-acting factor and not merely a structural element. ICU-BP, therefore, is likely to be an important component in cleavage of IGF-II mRNAs. However to confer endonucleolytic cleavage additional entities possibly interacting with the two additional stem–loops are required.

In Hep3B cells, the binding of ICU-BP to the stem structure is regulated in a growth-dependent manner. In cells grown to confluence the ICU-BP binding is 5-fold decreased as compared with exponentially growing cells. These differences in binding correlate inversely with the IGF-II mRNA levels (Fig. 7). Although the levels of 3′ cleavage product seem to increase along with the full length mRNA levels, this can still be consistent with a role for ICU-BP binding in cleavage of IGF-II mRNAs. Because many processes each with its own kinetics are occurring at the same time (promoter activities, differential stability of the mRNAs and the cleavage products) it is difficult to relate the observed steady state mRNA levels to one process in particular. With respect to the observed growth-related regulation it is interesting to note that translation of the 6.0 kb mRNA also appears to be dependent on the growth-status of the cells (28).

The physiological importance of ICU-BP is further indicated by the *in vivo* UV cross-linking experiments. UV cross-linking of intact cells has proven to be a powerful tool in the isolation of RNA-binding proteins (29–31). Only proteins that are very tightly associated with the RNA can be cross-linked. The efficiency of cross-linking is variable, depending on the protein and RNA involved (30). Recently, this technique was used in combination with an *in vitro* RNA-binding assay to show that AU-rich sequence binding proteins that bind *in vitro*, are also associated with the mRNA *in vivo* (24). UV-irradiation depletes ICU-BP from the transfected (e.g. IGF-II mRNA containing) cell line, but not from the non-transfected cell line. Because the presence or absence of IGF-II mRNA is the only difference between these cell lines this result suggests that also *in vivo* ICU-BP is associated with IGF-II mRNAs.

Some crude *in vitro* mRNA degradation systems have been reported (32–34), and components of degradation pathways have been identified, but neither of the two mRNA binding proteins involved in degradation that have been cloned to date, AUF1 (35) and IRP (36), are sufficient for the regulated degradation of their cognate mRNAs. For investigation of the function of ICU-BP in cleavage, an obvious experiment would be to purify the protein and test it in an *in vitro* cleavage assay. The resistance of the complex to high salt and its requirement for Mg^{2+} may aid in the purification of the protein. Cleavage of IGF-II mRNAs can be performed *in vitro*, but we have not yet succeeded in establishing an assay that is sufficiently reproducible (W. Scheper, unpublished data).

Our current working hypothesis for the mechanism of cleavage involves a functional relation between the formation of ICU-RPC and the level of IGF-II mRNA. In this model, formation of ICU-RPC facilitates the cleavage reaction and thereby the IGF-II mRNA degradation. However, formation of the ICU-RPC is not sufficient for cleavage and other proteins, possibly binding to the two additional stem–loops, are also required.

The function of the cleavage reaction is still elusive. It might be a first step in the degradation of IGF-II mRNAs, as has been suggested for other endonucleolytic cleavage reactions (37–39). Alternatively, the 3′ cleavage product may have some function in the cell by itself, since it is unusually stable for a cleavage product. Obviously, RNA can serve more functions than being an intermediate between the genome and the protein. In mammalian cells, effects of 3′ UTRs on differentiation and tumorigenesis were reported (40,41). If the 1.8 kb RNA exerts a function in the cell, its accumulation in the cytoplasm indicates that this is where to look for its action. Of course, these two possible functions of the cleavage reaction are not mutually exclusive.

In previous studies (20,21) we have identified the *cis*-acting elements involved in site-specific cleavage of human IGF-II mRNAs. In this study we initiated the characterization of *trans*-acting factors that play a role in this process, and have identified a novel protein, ICU-BP, that binds to the stem structure of IGF-II mRNAs. Future experiments will focus on: (i) the function and regulation of ICU-BP; to address this problem, an *in vitro* cleavage assay has to be developed; and (ii) the possible function of the 1.8 kb RNA. For the latter it will be interesting to investigate the effect of over-expression of the 1.8 kb RNA in cultured cells and transgenic animals.

ACKNOWLEDGEMENTS

We thank Tamás Henics for communicating data prior to publication, and Linda Nolten, Luc Rietveld and Richard Rodenburg for stimulating discussions.

REFERENCES

1 Sussenbach, J.S. (1989) *Progress Growth Factor Res.* **1**, 33–48.
2 Nielsen, F.C., Gammeltoft, S. and Christiansen, J. (1990) *J. Biol. Chem.* **265**, 13431–13434.
3 De Moor, C.H., Jansen, M., Sussenbach, J.S. and Van den Brande, J.L. (1994) *Eur. J. Biochem.* **222**, 1017–1022.
4 Nielsen, F.C. and Christiansen, J. (1992) *J. Biol. Chem.* **267**, 19404–19411.
5 Sachs, A.B. (1993) *Cell* **74**, 413–421.
6 Beelman, C.A. and Parker, R. (1995) *Cell* **81**, 179–183.
7 Ross, J. (1995) *Microbiol. Rev.* **59**, 423–450.
8 Sharp, P.A. (1994) *Cell* **77**, 805–815.
9 Keller, W. (1995) *Cell* **81**, 829–832.
10 Bernstein, P.L., Herrick, D.J., Prokipcap, R.D. and Ross, J. (1992) *Genes Dev.* **6**, 642–654.
11 You, Y., Chen, C.Y.A. and Shyu, A.B. (1992) *Mol. Cell. Biol.* **12**, 2931–2940.
12 Vakalopoulou, E., Schaack, J. and Shenk, T. (1991) *Mol. Cell. Biol.* **11**, 3355–3364.
13 Malter, J.S. (1989) *Science* **246**, 664–666.
14 Mullner, E.W., Neupert, B. and Kuhn, L.C. (1989) *Cell* **58**, 373–382.
15 Bohjanen, P.R., Petryniak, B., June, C.H., Thompson, C.B. and Lindsten, T. (1991) *Mol. Cell. Biol.* **11**, 3288–3295.
16 Wang, X., Kiledjian, M., Weiss, I.M. and Liebhaber, S.A. (1995) *Mol. Cell. Biol.* **15**, 1769–1777.
17 Jaffrey, S.R., Haile, D.J., Klausner, R.D. and Harford, J.B. (1993) *Nucleic Acids Res.* **21**, 4627–4631.
18 Dingwall, C., Ernberg, I., Gait, M.J., Green, S.M., Heaphy, S., Karn, J., Lowe, A.D., Singh, M. and Skinner, M.A. (1990) *EMBO J.* **9**, 4145–4153.
19 Kjems, J., Brown, M., Chang, D.D. and Sharp, P.A. (1991) *Proc. Natl Acad. Sci. USA* **88**, 683–687.
20 Meinsma, D., Scheper, W., Holthuizen, P.E. and Sussenbach, J.S. (1992) *Nucleic Acids Res.* **20**, 5003–5009.
21 Scheper, W., Meinsma, D., Holthuizen, P.E. and Sussenbach, J.S. (1995) *Mol. Cell. Biol.* **15**, 235–245.
22 Meinsma, D., Holthuizen, P.E., Van den Brande, J.L. and Sussenbach, J.S. (1991) *Biochem. Biophys. Res. Commun.* **179**, 1509–1516.
23 Li, Y., Ross, J., Scheppler, J.A. and Franza, B.R. (1991) *Mol. Cell. Biol.* **11**, 1883–1893.
24 Henics, T., Nagy, E. and Rigby, W.F.C. (1995) *Cell Biol. Int. Rep.* in press.
25 Chomczynski, P. and Sacchi, N. (1987) *Anal. Biochem.* **162**, 156–159.
26 Williams, M., Brys, A., Weiner, A.M. and Maizels, N. (1992) *Nucleic Acids Res.* **20**, 4935–4936.
27 Brewer, G. (1991) *Mol. Cell. Biol.* **11**, 2460–2466.
28 Nielsen, F.C., Ostergaard, L., Nielsen, J. and Christiansen, J. (1995) *Nature* **377**, 358–362.
29 Pelle, R. and Murphy, N.B. (1993) *Nucleic Acids Res.* **21**, 2453–2458.
30 Pinol-Roma, S., Adam, S.A., Choi, Y.D. and Dreyfuss, G. (1989) *Meth. Enzymol.* **180**, 410–418.
31 Wagenmakers, A.J.M., Reinders, R.J. and Van Venrooij, W.J. (1980) *Eur. J. Biochem.* **112**, 323–330.
32 Pastori, R.L. and Schoenberg, D.R. (1993) *Arch. Biochem. Biophys.* **305**, 313–319.
33 Brewer, G. and Ross, J. (1988) *Mol. Cell. Biol.* **8**, 1697–1708.
34 Brewer, G. and Ross, J. (1989) *Mol. Cell. Biol.* **9**, 1996–2006.
35 Zhang, W., Wagner, B.J., Ehrenman, K., Schaefer, A.W., DeMaria, C.T., Crater, D., DeHaven, K., Long, L. and Brewer, G. (1993) *Mol. Cell. Biol.* **13**, 7652–7665.
36 Rouault, T.A., Tang, C.K., Kaptain, S., Burgess, W.H., Haile, D.J., Samaniego, F., McBride, O.W., Harford, J.B. and Klausner, R.D. (1990) *Proc. Natl Acad. Sci. USA* **87**, 7958–7962.
37 Binder, R., Hwang, S.L., Ratnasabapathy, R. and Williams, D.L. (1989) *J. Biol. Chem.* **264**, 16910–16918.
38 Brown, B.D., Zipkin, I.D. and Harland, R.M. (1993) *Genes Dev.* **7**, 1620–1631.
39 Binder, R., Horowitz, J.A., Basilion, J.P., Koeller, D.M., Klausner, R.D. and Harford, J.B. (1994) *EMBO J.* **13**, 1969–1980.
40 Rastinejad, F. and Blau, H.M. (1993) *Cell* **72**, 903–917.
41 Rastinejad, F., Conboy, M.J., Rando, T.A. and Blau, H.M. (1993) *Cell* **75**, 1107–1117.